Published in final edited form as:
Biochem Pharmacol. 2010 November 1; 80(9): 1418–1426. doi:10.1016/j.bcp.2010.07.005.

Conformational flexibility of transmembrane helix VII of the human serotonin transporter impacts ion dependence and transport

Cody J. Wenthur, **Gustavo J. Rodríguez**[a], **Charles P. Kuntz**, and **Eric L. Barker**
Department of Medicinal Chemistry and Molecular Pharmacology, Purdue University School of Pharmacy and Pharmaceutical Sciences, West Lafayette, IN 47907-2091

Abstract

The serotonin transporter (SERT) regulates the serotonin concentration in the synapse and is a target of several antidepressant and psychostimulant drugs. Previous work suggested that the middle transmembrane helices (TMHs) of the biogenic amine transporters (TMHs) play a role in substrate and ion recognition. We focused our present studies on exploring the role of TMH VII in transporter function and ion recognition. Residues divergent between human SERT and *Drosophila* SERT (hSERT and dSERT, respectively) were identified and mutated in hSERT to the corresponding identity in dSERT. hSERT mutants V366S, M370L, S375A, and T381S exhibited a decrease in transport capacity. To further explore the role of these residues in the transport process, we generated cysteine mutants at multiple positions. Pretreatment with [2-(trimethylammonium)ethyl] methanethiosulfonate (MTSET) caused a decrease in transport of [^{3}H]5-HT in the V366C and M370C mutants. The hSERT V366S, M370L, and M370C mutations also altered the sodium and chloride dependence for substrate transport. Interpretation of our results in the context of a homology model of SERT based on the crystal structure of the *Aquifex aeolicus* leucine transporter suggests flexibility in the conformation of TMH VII that impacts ion dependence and substrate transport.

Keywords

cocaine; biogenic amine; amphetamine; protein structure

1. Introduction

The serotonin (5-hydroxytryptamine, 5-HT) transporter (SERT) is a plasma membrane protein that transports 5-HT from the synapse back into the cell. Several drugs selectively block the serotonin uptake mechanism and, to date, are the primary pharmacological method used to treat depression [1]. SERT is also a target of psychostimulants such as cocaine and amphetamines [2–4].

Corresponding Author: Eric L. Barker, Ph.D., Department of Medicinal Chemistry and Molecular Pharmacology, Purdue University School of Pharmacy, 575 Stadium Mall Drive, West Lafayette, IN 47907-2091, Office: 765-494-9940, Fax: 765-494-1414, barkerel@purdue.edu.
[a]Present/permanent address:
Verna and Marrs Department of Biochemistry and Molecular Biology, Baylor College of Medicine, One Baylor Plaza, N430 MS 125 Houston, TX 77030

Analysis of SERT shows high shared sequence identity with other members of the sodium- and chloride-dependent monoamine transporter family. Hydropathy studies predict twelve putative membrane-spanning α-helices, one of the topological signatures of this plasma membrane protein family [5–8]. The availability of the crystal structure of the *Aquifex aeolicus* leucine transporter ($LeuT_{Aa}$), a member of the Na+-dependent transporter family, provides a template for homology models of biogenic amine transporters [9–11]. The structure of $LeuT_{Aa}$ was crystallized in a "closed-closed" state with the substrate leucine forming contacts with TMHs I, III, VI, and VIII within the core mid-region of the transporter. Two Na^+ ions interact with $LeuT_{Aa}$ near the same TMHs coordinating leucine binding in the pore In addition, one of the two identified sodium sites involves TMH VII. The resolved structure of the $LeuT_{Aa}$ provides a wealth of information regarding the organization of TMHs in transporter proteins, albeit these structures only represent single-frame snapshots of the transport process and lack information on many of the contact sites involved with the conformational changes associated with substrate translocation.

Previously, the TMHs V to IX region of SERT and other monoamine transporters was implicated in substrate translocation and antagonist binding [12–18]. Previous work with cross-species chimeras from hSERT and dSERT identified the region between TMHs V and IX as important for observed differences in substrate transport [16] and antagonist binding [17;18]. Based upon the $LeuT_{Aa}$ structure, the potential role of TMHs VI–VIII in transporter function is worthy of exploration. The focus of the present studies is to determine the role of residues that diverge between hSERT and dSERT in the TMH VII region in the substrate transport and ion dependence process. Because TMH VII was shown to interact with Na^+ in the $LeuT_{Aa}$ structure [9], we considered the possibility that this domain may be critical for substrate translocation in SERT as well. Random mutagenesis of SERT in TMH VII identified critical residues for the sodium dependence of substrate transport [13]. In addition to its role in sodium dependence, TMH VII contains residues N368 and S372 that are involved in the formation of the Cl^- binding site [14;15]. Residues in a critical stripe region spanning from N368 to Y385 along one side of TMH VII have also been suggested to interact with other α-helices in SERT [16]. Thus, the complex role of TMH VII in the function of monoamine transporters could go beyond the information extracted from the $LeuT_{Aa}$ crystal structure.

To begin our analysis of TMH VII in ion recognition and substrate transport, we extended our cross-species chimera work with hSERT and dSERT by performing species-scanning mutagenesis [17;18]. Residues in TMH VII divergent between hSERT and dSERT were identified and mutated in hSERT to the residue identity found at the equivalent position in dSERT. TMH VII mutants, V366S, M370L, S375A and T381S, exhibited a reduction in 5-HT and *N*-methyl-4-phenylpyridinium (MPP^+) transport. Cysteine mutants at these positions in TMH VII were also generated with reactivity to methanethiosulfonates (MTS) revealing that residues V366 and M370 may be accessible from the external side of the transporter. Additional studies examining ion dependence of TMH VII mutants confirmed a role for this domain in sodium and chloride recognition. Interpretation of our data in the context of the $LeuT_{Aa}$ crystal structure suggests that TMH VII may have heretofore unrecognized flexibility and serve multiple roles in substrate translocation and ion recognition.

2. Materials and Methods

2.1 Materials

The cDNA encoding the C109A/hSERT mutant in pBluescript KSII was a generous gift from Dr. Randy Blakely (Vanderbilt University). [^{3}H]citalopram (85 Ci/mmol) was purchased from Amersham Biosciences Inc. (Piscataway, NJ). [^{3}H]MPP^+ (83.5 Ci/mmol) was obtained from PerkinElmer Life Sciences (Boston, MA). Fluoxetine, MPP^+, 3,4-methylenedioxymethamphetamine (MDMA) and pargyline were purchased from Sigma/RBI

(Natick, MA). MTSET and sodium (2-sulfonatoethyl)methane-thiosulfonate (MTSES), were purchased from Toronto Research Chemical (Toronto, Canada). Unlabeled 5-HT was obtained from Sigma-Aldrich (St. Louis, MO). All other reagents were purchased from commercial sources.

2.2 Cell culture

HEK-293 wild-type and transiently transfected cells were maintained in Dulbecco's Modified Eagle's Medium (DMEM) with 10% dialyzed fetal bovine serum supplemented with penicillin, streptomycin, and L-glutamine. Cells were grown in a 37°C humidified environment with 5% CO_2. Transient transfection was performed in 24-well poly-D-lysine coated plates using Lipofectamine 2000 per manufacturer's instructions (Life Technologies, Gaithersburg, MD).

2.3 Site-directed mutagenesis

Residues divergent between hSERT and dSERT in TMH VII were identified and mutated. We generated five mutants in the TMH VII region where the residue at hSERT was mutated to the identity at the corresponding position in dSERT. The mutants V366S, V367I, M370L, S375A, and T381S were generated using the QuikChange® site-directed mutagenesis kit (Stratagene, La Jolla, CA). Oligos were designed to introduce the mutation at the corresponding positions (Integrated DNA Technologies, Coralville, IA).

For SCAM we generated several cysteine mutants in TMH VII. The C109A/hSERT cDNA in pBluescript KSII was digested with NotI and AgeI enzymes. The resulting fragment was inserted in hSERT/pcDNA 3.1+ and digested with NdeI to confirm the C109A mutation. This cDNA was used as the background to generate all of the cysteine mutants in hSERT to reduce background methanethiosulfonate (MTS) reactivity [19]. Residues S365, V366, V367, M370, F380, and T381 were selected for mutation. Site-directed mutagenesis was performed using the QuikChange® mutagenesis kit as described above with the corresponding oligos. Mutations were confirmed by enzyme digestion and DNA sequencing (University of Michigan DNA sequencing core facility).

2.4 [^{3}H] Substrate uptake assays

Saturation transport assays were performed in 24-well culture plates precoated with poly-D-lysine. At the time of assay, transiently transfected (Lipofectamine 2000) HEK-293 cells (1×10^5 cells per well) were washed once with Krebs-Ringer-HEPES (KRH) buffer (120 mM NaCl, 4.7 mM KCl, 2.2 mM $CaCl_2$, 10 mM HEPES, 1.2 mM KH_2PO_4, 1.2 mM $MgSO_4$, pH 7.4). Cells were incubated with either single saturating concentrations or increasing concentrations of substrate (in the case of transport kinetic determinations) for 10 min at 37°C in KRH containing D-glucose (1.8 g/l), L-ascorbic acid (100 μM), and pargyline (100 μM). Saturating concentrations of substrate were determined based on previous studies [16;20]. In experiments examining antagonist potencies, increasing concentrations of antagonists were added 10 minutes prior to the addition of [^{3}H]5-HT. Fluoxetine (10 μM) was used to define nonspecific uptake. Assays were terminated by washing three times with KRH buffer, and the cells were solubilized in Microscint 20 (Perkin-Elmer, Waltham, MA). The amount of remaining radiolabeled substrate was then determined using a PerkinElmer TopCount-NXT Microplate Scintillation and Luminescence Counter.

For studies examining Na^+ dependence of 5-HT uptake, HEK-293 cells were plated and transiently transfected as above. Incubations were performed for 10 minutes at 37°C using KRH buffer and 100 nM [^{3}H]5-HT (100 Ci/mmol), where Na^+ was replaced by an equimolar concentration of Li^+ or *N*-methyl-D-glucamine (NMDG). For studies examining Cl^- dependence, Cl^- was replaced with an equimolar concentration of gluconate. Nonspecific

uptake, uptake termination, solubilization and counting of radiolabled substrate were performed as in the Na^+ dependence assays.

For uptake inhibition assays, transiently transfected HEK-293 cells were plated as described above. At the time of assay, the cells were washed with KRH buffer, incubated with increasing concentration of drug at 37°C for 10 min, and then treated with [^{3}H]5-HT (20 nM). Cells were incubated another 10 min at 37°C and uptake was terminated by washing three times with KRH buffer. Accumulated [^{3}H]5-HT was again determined using a PerkinElmer TopCount-NXT Microplate Scintillation and Luminescence Counter. V_{max} and K_m values in saturation experiments were calculated using nonlinear curve-fitting analysis (Prism 3.0; GraphPad Software Inc., San Diego, CA). Results were expressed as mean ± S.E.M. for at least three experiments performed in triplicate.

2.5 Cell surface radioligand binding assay

Cell surface radioligand binding experiments were performed in 24-well plates (1×10^5 cells per well) precoated with poly-D-Lysine as previously described [17]. This method exploits the membrane permeable radioligand [^{3}H]citalopram to define total binding (i.e., both surface and intracellular transporters). Two unlabeled ligands with differing membrane permeabilities, fluoxetine (membrane permeable) and MPP^+ (membrane impermeable), were used to define non-specific binding and intracellular and surface transporters, respectively.

The day after plating, cells were washed once with KRH. Cells were incubated with a saturating concentration (20 nM) of [^{3}H]citalopram at 4 C for 1 hour. Then, cells were rapidly washed twice with 1000 L KRH, solubilized with a 10% SDS solution, and transferred into a scintillation vial. Bound [^{3}H]citalopram was determined using a Beckman LS 1801 liquid scintillation counter (Irvine, CA). Total binding was established in the presence of KRH buffer. Nonspecific binding was defined as the binding of radiolabeled ligand in the presence of fluoxetine (10 μM). Internal binding was determined in the presence of MPP^+ (400 M).

2.6 Reactivity of cysteine mutants with MTS reagents

HEK-293 wild-type cells in 24-well tissue culture plates were transiently transfected with the cysteine mutant cDNAs of interest as described above. Following a 48-hour incubation, cells were washed once with PBS/CM buffer (137 mM NaCl, 2.7 mM KCl, 1.5 mM KH_2PO_4, 8.1 mM Na_2HPO_4, 0.1 mM $CaCl_2$, and 1.0 mM $MgCl_2$) and then incubated for 10 min at room temperature in the presence of an MTS reagent in PBS/CM buffer or buffer alone (total uptake). The concentrations of MTS reagents for investigating accessibility of cysteine mutants were as follows: 1 mM MTSET and 2 mM MTSES. Following MTS reagent treatment, cells were washed twice with PBS/CM and subjected to transport assays using 20 nM [^{3}H]5-HT or 50 nM [^{3}H]MPP^+ in KRH buffer. Nonspecific uptake was determined using 10 μM fluoxetine. Results were plotted using normalized data for each mutant, where the untreated activity levels are normalized to 100% to permit visualization of MTS sensitivity across different activity levels of the individual mutants. For MTS reagent treatment in the absence of Na^+, incubations were performed using KRH buffer instead of PBS/CM buffer, where NaCl was replaced by an equimolar concentration of LiCl. Protection assays were performed in a similar manner to the MTS treatments described above with the following changes: C109A/hSERT or TMH VII Cys mutants were incubated for 5 min at 25°C with buffer, 50 μM cocaine, 100 nM fluoxetine, 20 μM MDMA, 20 μM 5-HT, or 200 μM MPP^+ followed by incubation in the presence or absence of MTSET for 10 min. Saturating concentrations of the substrates or antagonist were used to ensure full occupancy of transporters during MTS incubations. The cells were washed three times with PBS/CM buffer to remove ligands and MTSET and then assayed for uptake activity as described above. The statistical importance of all results were determined using a one-way

ANOVA with a post-hoc Dunnett's multiple comparison test where $p < 0.05$ was determined to be significant.

2.7 Molecular Modelling

The initial model of hSERT was generated using the homology modeling program Modeller [21]. Atomic-resolution structures of mammalian biogenic amine transporters are currently not available, but the publication of the structure of the homologous leucine transporter from *Aquifex aeolicus* has allowed the generation of homology models of hSERT in which the amino acid sequence of the target is superimposed onto the tertiary structure of the $LeuT_{Aa}$ template. Modeller calculates protein structures by satisfaction of spatial restraints defined by the template, and also has a limited capacity to perform *ab initio* predictions in short loop regions. Sequence alignments between target and template proteins were adopted from Beuming [10], and the original leucine-bound structure of the leucine transporter served as the structural template (PDB 2A65) [9]. One thousand models of hSERT were generated, and the final model was chosen from among the ten best output structures as reported by the discrete optimized protein energy (DOPE) score, an atomic distance-dependent statistical potential used in the assessment of homology models [22]. Lower DOPE scores correlate with a distribution of distances between certain kinds of residues as observed in nature and are used here to select the best output from Modeller. Sodium and chloride ions were manually placed in their known positions, and serotonin was docked into the transporter using Autodock 4 [23], and 100 Lamarckian genetic algorithm docking runs were performed with an initial population size of 300 and a maximum of 25000000 evaluations . VMD was used to generate a 1-palmitoyl-2-oleoyl-phosphatidylcholine (POPC) (n=344) bilayer and water box surrounding the protein (125 Å × 125 Å × 105 Å) and add 150 mM NaCl. The entire system was then minimized using Gromacs [24] (steepest descent until convergence to Fmax < 1.000 kJ mol^{-1} nm^{-1}), and solvent equilibration was carried out for 2 ns with the full protein restrained, follow by 2 ns of equilibration with the side chains unrestrained. Finally, 40 ns molecular dynamics production runs with Particle-Mesh Ewald electrostatics and periodic boundary conditions were performed using the Amber force field (ffamber 03) ported to Gromacs.

3. Results

3.1 Mutations in TMH VII of hSERT affect substrate transport

Transport assays were performed on wild-type hSERT and each mutant using a saturating concentration of 5-HT or MPP^+ (20 μM and 200 μM, respectively) to measure transport capacity of these transporters (Fig. 1A and B). Mutants V366S, M370L, S375A, and T381S showed a decrease in transport activity for both substrates in comparison with wild-type hSERT (Fig. 1A and B). Transport kinetic experiments were performed and revealed that the K_m values for 5-HT and MPP^+ uptake at the mutants were similar to wild-type hSERT (data not shown).

To determine if the decrease of transport capacity in these mutants was due to lower surface expression, we performed whole-cell surface binding experiments [17]. Surface expression of mutants V366S, M370L, S375A, and T381S were lower than wild-type hSERT to varying degrees (Fig. 1C). Transport rates for each substrate were normalized to transporter surface expression to provide a measure of substrate turnover rate (Fig. 1D). This analysis revealed that the V366S, M370L, and T381S mutations reduced the turnover rate for both 5-HT and MPP^+ although 5-HT turnover appeared more significantly impacted than MPP^+. Interestingly, the 5-HT turnover rate at the S375A mutant was comparable to wild-type hSERT whereas MPP^+ turnover was reduced by ~75% (hSERT 0.3×10^{-13} nMoles/min/transporter vs. S375A 0.08×10^{-13} nMoles/min/transporter). Despite the changes in turnover for substrate transport, the hSERT mutations did not significantly alter antagonist potencies (Table 1).

3.2 V366C and M370C mutants are accessible to MTSET and partially protected by substrates

Based on our SERT homology model based on the $LeuT_{Aa}$ structure, residues V366, M370, and T381 are predicted to face the same side of the α-helix on TMH VII that is oriented toward the lipid bilayer, whereas S375 is predicted to be localized on the other side of TMH VII. To further explore the role of these residues in the transport process, we generated cysteine mutants at positions S365, V366, V367, M370, S375, F380, and T381. The S365, V367, and F380 positions were mutated in addition to V366, M370, S375, and T381 to probe possible roles of neighboring residues on the helix of TMH VII. Studies at wild-type hSERT using MTS reagents have demonstrated that the native cysteine at position 109, localized in the first extracellular loop, is sensitive to MTS reagents [19]. For our studies, we used the C109A/hSERT mutant as a background to generate the TMH VII cysteine mutants to avoid possible influences of native cysteines in the SERT structure.

[^{3}H]5-HT transport assays revealed similar uptake capacity for S365C, V367C, and S375C in comparison with C109A/hSERT (Fig. 2A). Two mutants, F380C and T381C, showed approximately 50% reduction in 5-HT transport. Mutants V366C and M370C showed the greatest loss of transport capacity with approximately 5% of C109A/hSERT transport. Likewise, we performed transport assays in these mutants using [^{3}H]MPP^+. V366C and M370C showed the greatest reduction in MPP^+ transport in comparison to C109A/hSERT (Fig. 2B). S365C, V367C, or F380C did not exhibit statistically different MPP^+ transport with respect to C109A/hSERT. Interestingly, the S375C mutant showed a 50% reduction in MPP^+ transport. This mutation did not affect 5-HT transport supporting our previous results with the S375A mutant (Fig. 1).

We used membrane-impermeable MTS reagents to determine the accessibility of the cysteine mutants to the hydrophilic environment and to address the possibility that these residues may be part of the pore-forming region in SERT. Pretreatment with MTSET (Fig. 3A and B) or MTSES (data not shown) caused a decrease in [^{3}H]5-HT transport capacity for V366C (approximately 25% reduction) and M370C (approximately 55% reduction). Furthermore, MTSET reactivity was reduced by incubation with unlabeled 5-HT (20 μM) or MPP^+ (200 μM) at the V366C mutant, but not at the hSERT M370C mutant (Fig. 3A and 4B). These results suggest that both V366C and M370C are accessible to the external environment in a region that may be impacted by substrate translocation.

Assays similar to those outlined above were performed in sodium-free buffer (Fig. 3C and D). Previous SCAM experiments with cysteine mutants showed an increase in MTSET reactivity of the C109A/hSERT mutant in the absence of Na^+ [19]. Sodium is a key component for substrate transport by SERT. Upon sodium binding, changes in conformation of SERT may alter accessibility of cysteine residues [25]. To determine if sodium alters the accessibility of V366C or M370C, we replaced sodium with an equimolar concentration of lithium, thus, maintaining the buffer's ionic strength. Sodium-free buffer was used only during the pretreatment with MTS reagents. Lithium-containing buffer did not alter accessibility of V366C, M370C, or other TMH VII cysteine mutants to MTSET (Fig. 3C and D), similar to what we observed using sodium-containing buffer (Fig. 3A and B). One difference observed when sodium was replaced by lithium was the gain of partial protection by substrates at the M370C mutant and the loss of protection by MPP^+ at the V366C mutant. We attempted uptake studies using [^{3}H]MPP^+ as a substrate in the V366C and M370C mutants, but due to the low transport capacity of MPP^+ by these SERT mutants (Fig. 2B), the effects of MTSET on MPP^+ transport were not detected. Other mutants did not show statistically significant differences in MPP^+ transport capacity upon MTSET treatment in comparison to C109A/hSERT (data not shown).

We also explored the ability of various SERT ligands including fluoxetine, cocaine, and MDMA to protect the V366C and M370C mutants from MTSET accessibility. The cysteine mutations at positions V366 and M370 did not alter the K_i values for these drugs in comparison with C109A/hSERT (data not shown). Coincubation of saturating concentrations of these drugs completely protected both mutants from MTSET inactivation (Fig. 4). The SERT antagonists fluoxetine and cocaine as well as the substrate MDMA were able to protect V366C from MTSET interaction, similar to 5-HT and MPP^+. Interestingly, these drugs also protected M370C, whereas 5-HT and MPP^+ did not protect M370C from MTSET inactivation when assayed in Na^+-containing buffer.

3.3 hSERT V366 and M370 mutants display altered sodium and chloride dependence for 5-HT transport

As residues V366 and M370 are predicted to be in proximity to residues involved in sodium binding [9], we probed the sodium dependence of 5-HT transport for the V366C, V366S, M370C, and M370L mutants. When Na^+ was replaced with Li^+, the control C109A/hSERT demonstrated sodium-dependent transport and a kinetic profile consistent with one-site binding (Fig. 5A). The V366C mutant also exhibited kinetics consistent with one-site binding and had a similar K_m to that of C109A. Low levels of activity were associated with the V366S mutant, with its observed maximum uptake occurring between 75 and 125 mM Na^+ and reduced transport at Na^+ concentrations greater than 125 mM (Fig. 5B). The M370C mutant exhibited altered sodium dependence for transport displaying a bi-phasic property and maximum uptake occurring between 25 and 50 mM Na^+. Additionally, mutant M370L had low levels of activity, in a range similar to that of V366S, but showed maximum activity between 35 and 75 mM Na^+ (Fig. 5C).

In order to explore altered ion dependence of these mutants further, the V366 and V370 mutants were examined in the same experimental conditions as described above, excepting that Na^+ was replaced with an equimolar concentration of NMDG rather than Li^+. With NMDG replacing Na^+, the control C109A/hSERT again showed kinetics consistent with one-site binding (Fig. 5D). Mutant V366C again followed the activity pattern of C109A/hSERT, but with a maximal activity ~50% less than that observed with the Li^+ substitution condition. Mutants V366S, M370C, and M370L exhibited minimal activity for all tested concentrations of Na^+ under the NMDG substitution conditions (Figs. 5E and 5F).

Residues N368 and S372 have been implicated in forming part of the chloride ion binding site in SERT, so we tested hSERT mutants at proximal residues V366 and M370 to examine Cl^- dependence of 5-HT transport [14;15]. In this condition, gluconate was substituted for Cl^- at equimolar concentrations. C109A/hSERT demonstrated one-site binding kinetics (Fig. 6A). V366C again showed a similar kinetic profile to C109A/hSERT (Fig. 6B). V366S demonstrated low levels of activity in this condition. However, the activity remaining was marked with a bi-phasic property, and maximal activity was observed between 35 and 75 mM Cl^- (Fig. 6B [inset]). Mutant M370C presented little activity across all tested Cl^- concentrations, and mutant M370L had a kinetic profile consistent with one-site binding for Cl^- dependence (Fig. 6C).

4. Discussion

Different TMHs and extracellular loops of SERT have been implicated for ion recognition and transport. Among them, TMH VII has been the focus of several studies. In our studies, functional assays performed on the mutants identified four mutations (V366S, M370L, S375A, and T381S) that decreased transport capacity for the two substrates tested, 5-HT and MPP^+. Comparison of the transport of 5-HT and MPP^+ can reveal a shift in phenotype toward dSERT as the *Drosophila* transporter is incapable of transporting MPP^+ [17]. If a particular mutation

in hSERT selectively affects the transport of a specific substrate, this would be revealed by a greater mutation-induced impact on transport of that substrate. For example, three mutations V366S, M370L, and T381S exhibited greater loss of 5-HT uptake compared to MPP^+ uptake in comparison to wild-type hSERT. Interestingly, for the S375A mutant the opposite was observed, as MPP^+ uptake was reduced by nearly 75% compared to 5-HT transport at hSERT, revealing a more pronounced mutation-induced effect on MPP^+ transport. Analysis of the predicted orientation of TMH VII based on the SERT homology model localized residues V366, M370, and T381 to the same face of the α-helix, whereas S375 is predicted to be on the opposite side. According to the homology model, residues V366, M370, and T381 appear to orient toward the lipid bilayer (Fig. 7). This prediction follows from the alignment with the leucine transporter in the region of TMH VII. The alignment was adopted from a previously published comprehensive structure-based alignment of known neurotransmitter:sodium symport transporters [10].

A number of residues in TMH VII are conserved across the entire family, including hSERT I379 ($LeuT_{Aa}$ I297), which is one helical turn away from S275, and more are conserved in eukaryotic transporters, including hSERT S372, which has been determined to be a key residue in the hSERT chloride binding site. Mutation of the homologous $LeuT_{Aa}$ residue E290 to serine caused $LeuT_{Aa}$ to be chloride-dependent, whereas mutation of hSERT S372 yielded a transporter that catalyzes transport independently of chloride concentration [15]. Our alignment is similar to the alignment used in that study, and our homology model shows S372 occupying the same position thought necessary to coordinate with chloride, one helical turn above N368, which coordinates with both chloride and sodium. Perhaps mutations of the nearby residues V366, M370, and S375 alter the conformation of TMH VII in a manner similar to mutation of S372E, decoupling substrate transport with ion bound at the chloride binding site. A negative charge at the position of S372 is thought to participate in a local network of interactions that gate neurotransmitter transport; mutations in these nearby residues on the helix may disrupt this network in a manner that affects gating. In our molecular dynamics studies, there is considerable movement of TMH VII at the residues M370 and S375. For example, at the 3 ns simulation the distance between the beta carbon of S375 and the phenolic oxygen of Y289 on the adjacent TMH V is 5.8 Å, whereas 20 ns later this distance is 8.5Å (Figure 7). This change in distance may reflect an inherent flexibility in this region that is disrupted or altered upon mutation. This flexibility may be necessary for chloride binding and, ultimately, transport. These mutants exhibited lower cell surface expression in comparison to wild-type hSERT explaining reduced 5-HT transport and suggesting that these mutations may also affect SERT trafficking to the plasma membrane.

To further address the role of TMH VII in transporter function, we generated cysteine mutants at position S365, V366, V367, M370, S375, F380, and T381. These mutations were selected to explore different regions in the helix that could be exposed to the hydrophilic environment. SCAM studies using the membrane-impermeable MTSET revealed reactivity with only mutants V366C and M370C. These results suggest that V366 and M370 residues are exposed to the hydrophilic environment and reactivity with MTS is able to disrupt transport. In the presence of Na^+, coincubation of unlabeled 5-HT or MPP^+ was able to protect V366C, but not the M370C mutant, from MTSET interaction. However, when Na^+ was replaced with Li^+, and thus, preventing transport, unlabeled 5-HT was able to partially protect the M370C mutant from MTSET interaction. The topology of SERT predicts that V366 is localized deeper in the pore than M370, thus, possibly impacting the ability of 5-HT to protect only the V366C mutant. One possibility is that an important 5-HT binding site resides deeper in the pore making V366 closer to the contact site than M370, although there is no evidence that V366 has direct contact with 5-HT. The localization of V366C deeper in the pore makes this residue more likely to be protected from inactivation by MTSET during 5-HT translocation than M370C. This model is supported by the observation that in the presence of Li^+, a condition where 5-HT can still bind

to the transporter but not trigger translocation, the V366C and M370C mutants are partially protected by 5-HT. However, in the presence of Na^+ and 5-HT, only the residue deeper in the pore (V366) is protected from MTSET inactivation. As these protective effects of substrates for MTSET inactivation could be due to changes in SERT conformation, further investigation of these residues is necessary to confirm the direct nature of their influences on substrate recognition.

The SERT ligands fluoxetine, cocaine, and MDMA also were able to protect V366C and M370C from MTSET inactivation. Our findings suggest that M370 and V366 residues could be in close proximity to the binding site for these drugs, and therefore upon antagonist binding, these sites are protected from interacting with MTSET. We must also consider the possibility that these drugs could induce conformational changes that prevent the accessibility of these residues from interacting with MTSET. This possibility is supported by a study in DAT that identified determinants in TMHs VII and VIII for cocaine-dependent conformational changes [25].

The other TMH VII cysteine mutants did not show sensitivity to MTSET. Although in the first set of experiments mutation of residues S375 and T381 to their counterparts in dSERT suggested that these residues were able to impact transport, SCAM analysis at these positions did not show MTSET inactivation. One possible explanation is that S375 and T381 form interactions with other TMHs necessary for the conformational changes required for substrate translocation. Indeed, a homology model of hSERT derived from the crystal structure of $LeuT_{Aa}$ [9] reveals that S375 and T381 could form hydrogen bonds with Thr371 or Tyr289 (TMH V) and Tyr110 (TMH I), respectively. From our studies we cannot also rule out the possibility that MTSET was inaccessible to S375C or T381C mutants due to a steric constraint in this region or unfavorable interaction with the positively-charged MTSET.

Previously, random mutagenesis studies in TMH VII identified five residues (N368, F373, F377, F380, and Y385) that form a stripe suggested to be important for the translocation of 5-HT and ions [13]. The stripe of residues down TMH VII was the subject of further analysis to determine their role in SERT function. SCAM provided evidence that these residues are necessary for the propagation of conformational changes occurring after ion binding to the transporter [16]. Perhaps this domain is an essential part of the translocation mechanism as the identified stripe region is likely to represent a close contact site for TMH VII and one or more other TMHs.

Our homology model of hSERT proposes that position N368 is predicted to form part of a Na^+ binding site (Fig. 7). Based on this structural information, TMHs I and VI also participate in the binding of the Na^+ (Fig. 7). N368, along with S372, has been suggested to be important for the binding of Cl^- as well [14;15]. We propose that the alterations in Na^+ and Cl^- dependence for the hSERT V366 and M370 mutants (T284 and K288 in $LeuT_{Aa,}$ respectively) are a result of mutation-induced secondary influences on hSERT N368 and hence the binding of these ions to SERT. Our data suggest that higher Na^+ concentrations interfere with transport activity in the V366S and M370C mutants. One explanation for our results is that the mutations may have altered the Na^+ binding site such that at high concentrations, Na^+ either directly blocks the transport permeation pathway or stabilizes the transporter in such a way to prevent conformations necessary for substrate translocation. This issue is further complicated by our homology model which suggests that the more exterior portion of the TMH VII α-helix may be able to unwind (Fig. 7) providing additional capability of this helix to potentially rotate. The cysteine mutations may alter the orientation of the helix, making these positions accessible to MTSET and at the same time rotating N368 and S372 away from the Na^+ and Cl^- binding sites. Such rotation of TMH VII would explain the accessibility of these otherwise occluded residues to MTSET and the altered transport via disruption of ion binding.

Taken together, our results suggest a complex role of SERT TMH VII in the function of SERT. The SERT homology model based on the $LeuT_{Aa}$ crystal structure and our functional data support a role of TMH VII in Na^+ and Cl^- dependence of 5-HT transport. Interestingly, V366 and M370 are predicted to reside on the face of the helix opposite the Na^+ binding site, and thus, interface with the membrane bilayer (Fig. 7), yet these residues are able to become accessible to cysteine-modifying reagents. One interpretation of these results suggests that following Na^+ binding and inward transport, TMH VII could rotate to make the V366 and M370 face of the helix accessible to the substrate permeation pathway. The Na^+ and Cl^- binding sites, which include N368 as discussed above, reside near the substrate binding site observed in the closed-closed state of the $LeuT_{Aa}$ crystal structure [9]. During translocation, however, there is no requirement for these ion and substrate binding site proximities to be maintained. Indeed, we suggest that movement of Na^+ could precede a rotation in TMH VII making the V366 and M370 face of this helix accessible. Our results suggest that V366 and M370 mutations have the ability to interrupt ion binding occurring at this site and cause a reorientation of the TMH VII α-helix which prevents such a rotation from occurring, and thus, lead to decreased substrate transport. These results represent a potential molecular mechanism for the contributions of TMH VII to substrate translocation and ion dependence.

Acknowledgments

The authors thank Dr. Randy D. Blakely (Vanderbilt University) for providing the C109A/hSERT pBluescript KSII plasmid. This work was supported by the National Institute on Drug Abuse DA018682 (E.L.B.) and American Psychological Association Minority Fellowship program (G.J.R.).

References

1. Jacobs, BL.; Fornal, CA. Serotonin and behavior: A general hypothesis. In: Bloom, F.; Kupfer, D., editors. Psychopharmacology: The Fourth Generation of Progress. Raven Press; New York: 1995. p. 461-9.
2. Rudnick G, Wall SC. p-Chloroamphetamine induces serotonin release through serotonin transporters. Biochemistry 1992;31:6710–18. [PubMed: 1322169]
3. Rudnick G, Wall SC. The molecular mechanism of “ecstasy”: serotonin transporters are targets for MDMA-induced serotonin release. Proc Natl Acad Sci US A 1992;89:1817–21.
4. Wall SC, Gu H, Rudnick G. Biogenic amine flux mediated by cloned transporters stably expressed in cultured cell lines: amphetamine specificity for inhibition and efflux. Mol Pharmacol 1995;47:544–50. [PubMed: 7700252]
5. Blakely RD, Berson HE, Fremeau RTJ, Caron MG, Peek MM, Prince HK, Bradley CC. Cloning and expression of a functional serotonin transporter from rat brain. Nature 1991;354:66–70. [PubMed: 1944572]
6. Hoffman BJ, Mezey E, Brownstein MJ. Cloning of a serotonin transporter affected by antidepressants. Science 1991;254:579–80. [PubMed: 1948036]
7. Ramamoorthy S, Bauman AL, Moore KR, Han H, Yang Feng T, Chang AS, Ganapathy V, Blakely RD. Antidepressant- and cocaine-sensitive human serotonin transporter: molecular cloning, expression, and chromosomal localization. ProcNatlAcadSciUS A 1993;90:2542–6.
8. Demchyshyn LL, Pristupa ZB, Sugamori KS, Barker EL, Blakely RD, Wolfgang WJ, Forte MA, Niznik HB. Cloning, expression, and localization of a chloride-facilitated cocaine-sensitive serotonin transporter from Drosophila melanogaster. ProcNatlAcadSciUS A 1994;91:5158–62.
9. Yamashita A, Singh SK, Kawate T, Jin Y, Gouaux E. Crystal structure of a bacterial homologue of Na+/Cl--dependent neurotransmitter transporters. Nature 2005;437:203–5. [PubMed: 16148921]
10. Beuming T, Shi L, Javitch JA, Weinstein H. A Comprehensive Structure-Based Alignment of Prokaryotic and Eukaryotic Neurotransmitter/Na+ Symporters (NSS) Aids in the Use of the LeuT Structure to Probe NSS Structure and Function. Mol Pharmacol 2006;70:1630–42. [PubMed: 16880288]

11. White KJ, Kiser PD, Nichols DE, Barker EL. Engineered zinc-binding sites confirm proximity and orientation of transmembrane helices I and III in the human serotonin transporter. Protein Sci 2006;15:2411–22. [PubMed: 17008722]
12. Kitayama S, Shimada S, Xu H, Markham L, Donovan DM, Uhl GR. Dopamine transporter site-directed mutations differentially alter substrate transport and cocaine binding. ProcNatlAcadSciUS A 1992;89:7782–5.
13. Penado KMY, Rudnick G, Stephan MM. Critical amino acid residues in transmembrane Span 7 of the serotonin transporter identified by random mutagenesis. J Biol Chem 1998;273:28098–106. [PubMed: 9774428]
14. Zomot E, Bendahan A, Quick M, Zhao Y, Javitch JA, Kanner BI. Mechanism of chloride interaction with neurotransmitter:sodium symporters. Nature 2007;449:726–30. [PubMed: 17704762]
15. Forrest LR, Tavoulari S, Zhang YW, Rudnick G, Honig B. Identification of a chloride ion binding site in Na+/Cl -dependent transporters. Proc Natl Acad Sci USA 2007;104:12761–6. [PubMed: 17652169]
16. Kamdar G, Penado KMY, Rudnick G, Stephan MM. Functional role of critical stripe residues in transmembrane Span 7 of the serotonin transporter. J Biol Chem 2001;276:4038–45. [PubMed: 11058600]
17. Rodriguez GJ, Roman DL, White KJ, Nichols DE, Barker EL. Distinct recognition of substrates by the human and Drosophila serotonin transporters. JPharmacolExp Ther 2003;306:338–46.
18. Roman DL, Walline CC, Rodriguez GJ, Barker EL. Interactions of antidepressants with the serotonin transporter: a contemporary molecular analysis. Eur J Pharmacol 2003;479:53–63. [PubMed: 14612137]
19. Chen JG, Liu-Chen S, Rudnick G. External cysteine residues in the serotonin transporter. Biochemistry 1997;36:1479–86. [PubMed: 9063896]
20. Norregaard L, Loland CJ, Gether U. Evidence for distinct sodium-, dopamine-, and cocaine-dependent conformational changes in transmembrane segment 7 and 8 of the dopamine transporter. J Biol Chem 2003;278:30587–96. [PubMed: 12773538]
21. Fiser A, Sali A. Modeller: Generation and Refinement of Homology-Based Protein Structure Models. Method Enzymol 2003;374:461–491.
22. Shen MY, Sali A. Statistical potential for assessment and prediction of protein structures. Protein Sci 2006;15:2507–2524. [PubMed: 17075131]
23. Morris GM, Huey R, Lindstrom W, Sanner MF, Belew RK, Goodsell DS, Olsen AJ. AutoDock4 and AutoDockTools4:Automated docking with selective receptor flexibility. J Comp Chem 2009;16:2785–91. [PubMed: 19399780]
24. Van Der Spoel D, Lindahl E, Hess B, Groenhof G, Mark A, Berendsen JC. GROMACS: Fast, Flexible, and Free. J Comp Chem 2005;16:1701–18. [PubMed: 16211538]
25. Ni YG, Chen J-G, Androutsellis-Theotokis A, Huang C-J, Moczydlowski E, Rudnick G. A lithium-induced conformational change in serotonin transporter alters cocaine binding, ion conductance, and reactivity of Cys-109. J Biol Chem 2001;276:30942–7. [PubMed: 11408487]

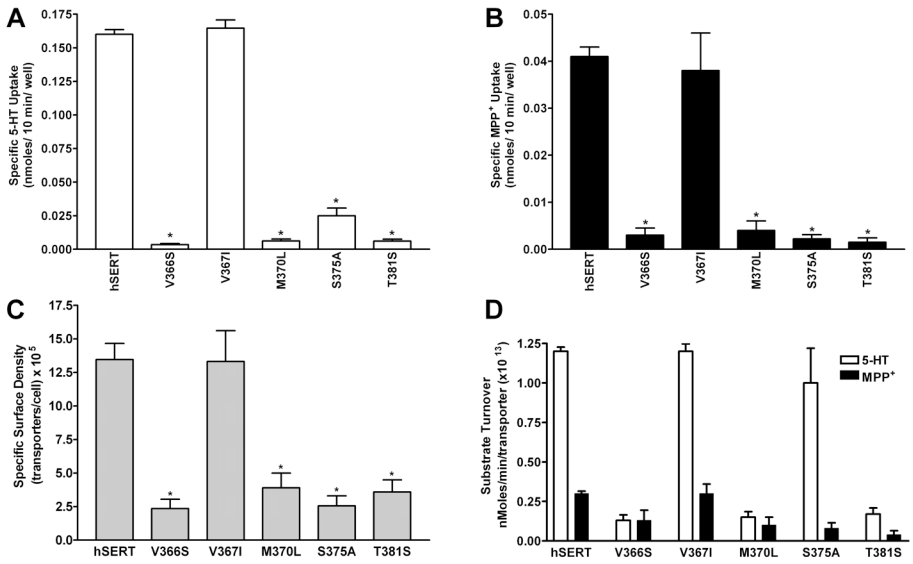

Figure 1.

Uptake of (A) 5-HT and (B) MPP+ in HEK-293 cells transiently transfected with hSERT or hSERT mutants. Cells were plated and transfected as described in Materials and Methods. Saturating concentrations of [^{3}H]5-HT (20 μM) or [^{3}H]MPP$^+$ (200 μM) were achieved by diluting specific activity to ~0.1 Ci/mmol with non-isotopic compound. Non-specific uptake was determined using fluoxetine (10 μM). Bars represent the mean of three independent experiments SEM, *, p <0.05 using a one-way ANOVA test with a post-hoc Dunnett's multiple comparison test as compared to hSERT. (C), Whole-cell radioligand binding in HEK-293 cells transiently transfected with wild-type or hSERT mutants. Assays were performed in 24-well plates coated with poly-D-Lysine as described under Materials and Methods. A saturating concentration of [^{3}H]citalopram (20 nM) was used for hSERT and mutants. Nonspecific binding was defined as the binding of radiolabeled ligand in the presence of 10 μM fluoxetine. Internal binding was determined as the binding of [^{3}H]citalopram in the presence of 400 μM MPP$^+$. Specific surface binding was calculated as (total binding – binding in the presence fluoxetine) –(binding in the presence of MPP$^+$ – binding in the presence of fluoxetine). Transporter molecules were calculated assuming one citalopram bound per transporter. Bars represent the mean of three independent experiments ± SEM. *, p < 0.05 using a one way ANOVA with post-hoc Dunnett's multiple comparison test as compared to hSERT. (D) Substrate turnover rates calculated by dividing transport rates (A) and (B) by transporter surface density (C).

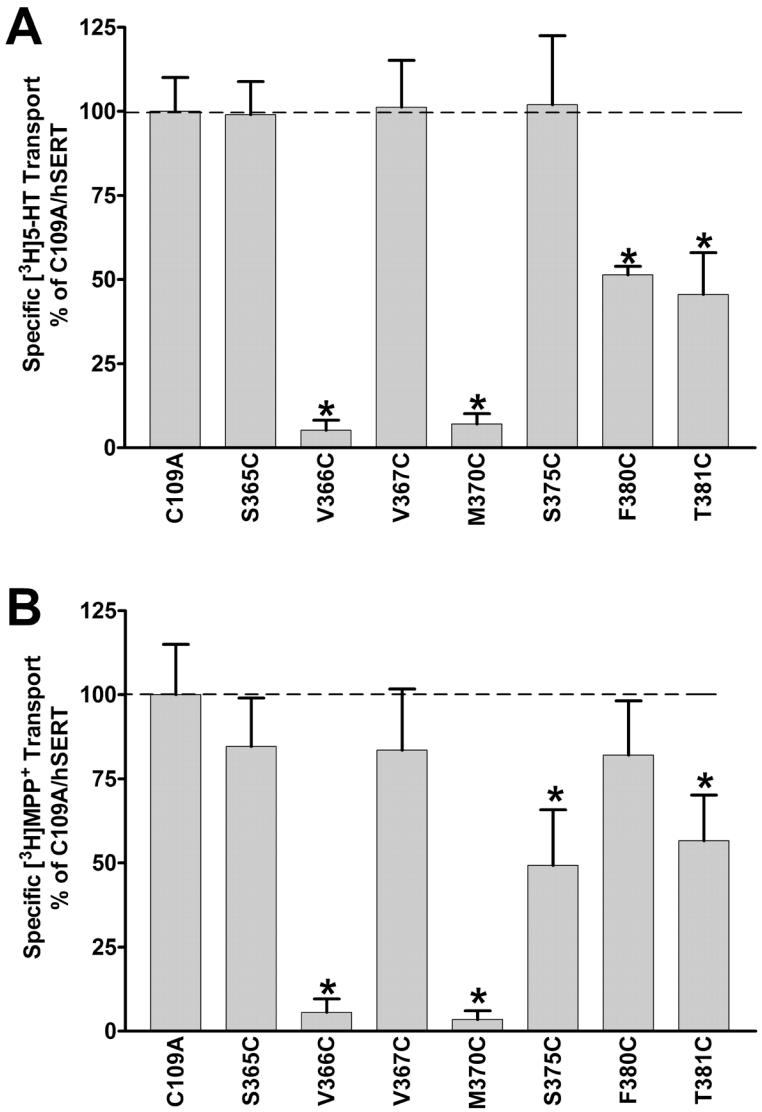

Figure 2.

Transport activity of SERT cysteine mutants in TMH VII. C109A/hSERT and TMH VII mutants were transiently transfected in HEK-293 cells as described in Material and Methods. (A) Transport activity in the presence of [^{3}H]5-HT (20 nM) for 10 min. (B) Transport activity in the presence of [^{3}H]MPP$^+$ (50 nM) for 10 min. Bars represent mean ± SEM from three experiments performed in triplicate. *, $p < 0.05$ using a one way ANOVA with a post-hoc Dunnett's multiple comparison test as compared to C109A/hSERT.

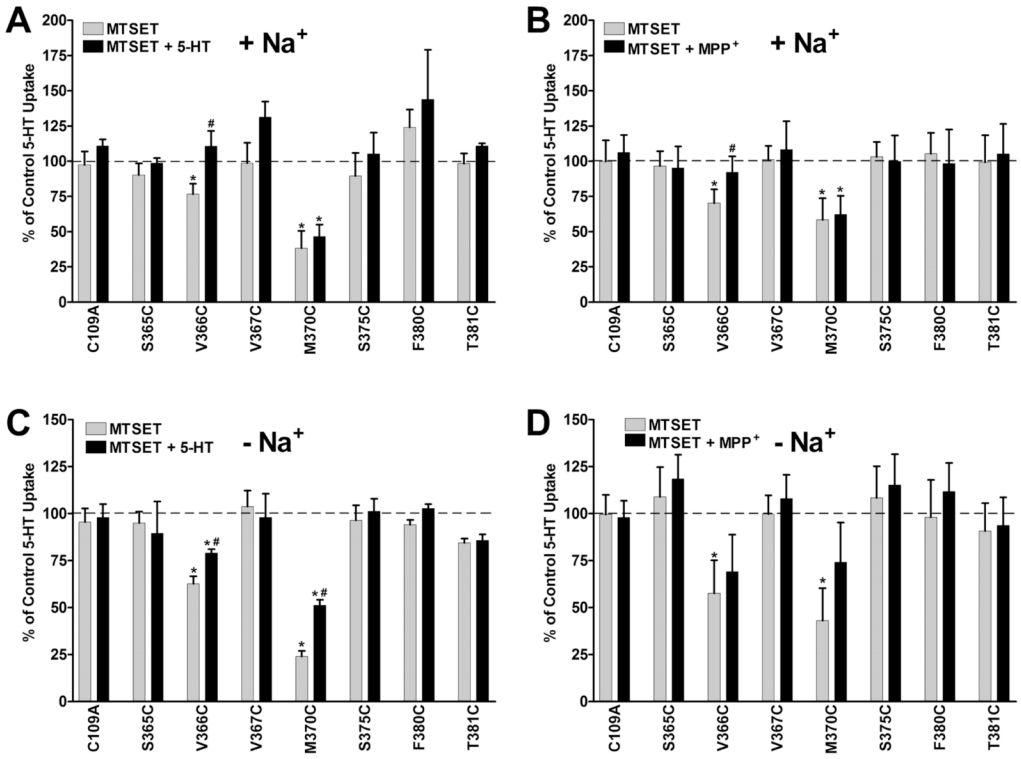

Figure 3.

Effects of MTSET on the inactivation of [^{3}H]5-HT transport in HEK-293 transiently transfected cells with C109A/hSERT or Cys-mutants. 48-hours after transfection, cells were preincubated with MTSET (1 mM) for 10 minutes at room temperature followed by [^{3}H]5-HT (20 nM) uptake as described in Materials and Methods. Preincubation with MTSET was performed in the presence of: (A) PBS/CM buffer ± 20 μM unlabeled 5-HT, (B) PBS/CM buffer ± 200 μM unlabeled MPP^+, (C) KRH/sodium-free buffer ± 20 μM unlabeled 5-HT, or (D) KRH/sodium-free buffer ± 200 μM unlabeled MPP^+. NaCl was replaced with equimolar concentration of LiCl to maintain the buffer's ionic strength. Unlabeled substrate was used to determine the ability to protect the mutants from MTS-inactivation. Bars represent mean ± SEM from three experiments performed in triplicate. *, $p < 0.05$ using a one way ANOVA with a post hoc Dunnett's multiple comparison test as compared to C109A/hSERT control. #, $p < 0.05$ as compared to MTSET treatment.

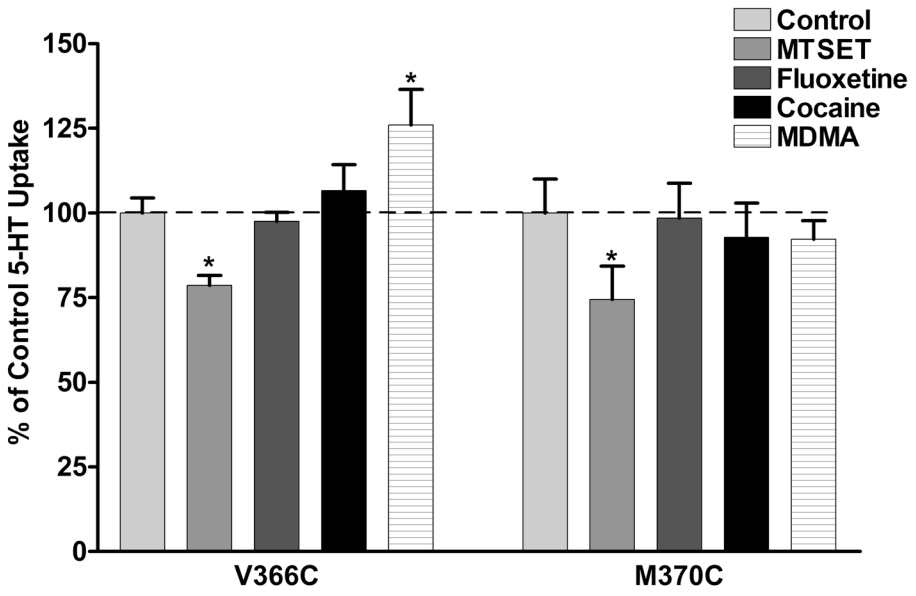

Figure 4.

MTSET accessibility and protection assays using fluoxetine, cocaine, and MDMA in HEK-293 cells transiently transfected with hSERT V366C or M370C mutant cDNAs. Saturating concentrations of fluoxetine (100 nM), cocaine (200 μM), or MDMA (200 μM) were coincubated with MTSET (1 mM) for 10 minutes at room temperature. Nonspecific transport was determined in the presence of fluoxetine (10 μM). After MTSET/antagonist pretreatment, cells were washed three times with PBS/CM buffer to remove the drugs prior to the substrate transport assay. Cysteine mutants at positions V366 and M370 did not alter the K_i values for 5-HT transport inhibition of these drugs (data not shown). Bars represent mean ± SEM for three independent experiments performed in triplicate. *, $p < 0.05$ using a one way ANOVA with a post-hoc Dunnett's multiple comparison test as compared to buffer control.

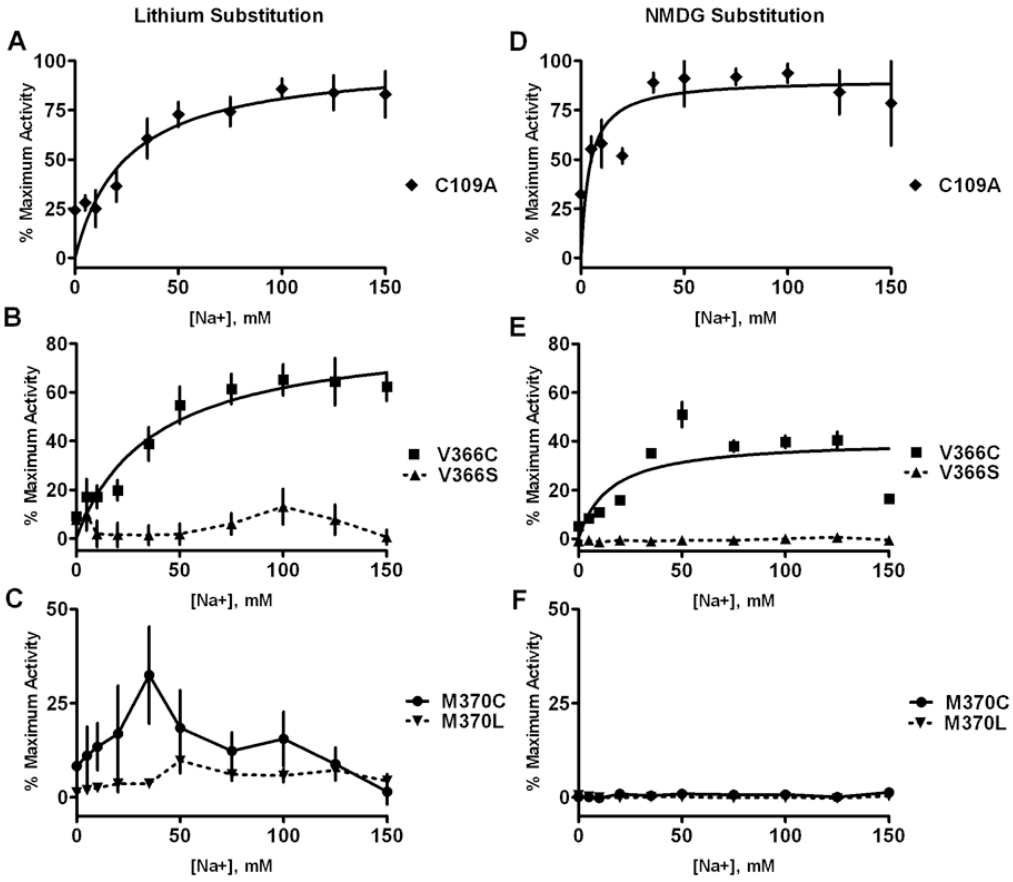

Figure 5.

Sodium dependence of [^{3}H]5-HT transport for V366C, V366S, M370C, and M370L mutants. Cells were plated and transfected as described in Materials and Methods. Incubations were performed using KRH buffer, where Na^+ was replaced by an equimolar concentration of Li^+ (Panels A–C), or by NMDG (Panels D–F). Nonspecific transport was determined in the presence of fluoxetine (10 μM). Data are representative of three experiments performed in triplicate. K_m values for Na^+ in the presence of lithium were determined for mutants C109A/hSERT (24.6 ± 7.7 mM) and V366C (37.7 ± 12.7 mM). K_m values for Na^+ were also determined in the presence of NMDG for C109A/hSERT (4.1 ± 1.8 mM) and V366C (15 ± 5.6 mM). None of the other conditions produced measurable K_m values.

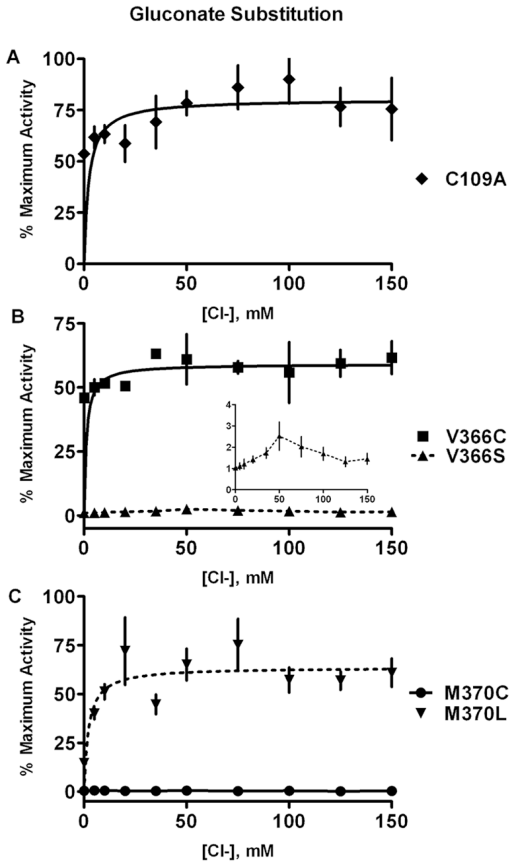

Figure 6.

Chloride dependence of [3H]5-HT transport for V366C, V366S, M370C, and M370L mutants. Cells were plated and transfected as described in Materials and Methods. Incubations were performed using KRH buffer, where Cl^- was replaced by an equimolar concentration of gluconate. Nonspecific transport was determined in the presence of fluoxetine (10 μM). Data are representative of three experiments performed in triplicate. K_m values for Cl^- were determined for mutants C109A/hSERT (2.2 ± 1.7 mM), V366C (1.1 ± 1.0 mM), and M370L (2.2 ± 1.6 mM) in the presence of gluconate. None of the other conditions produced measurable K_m values.

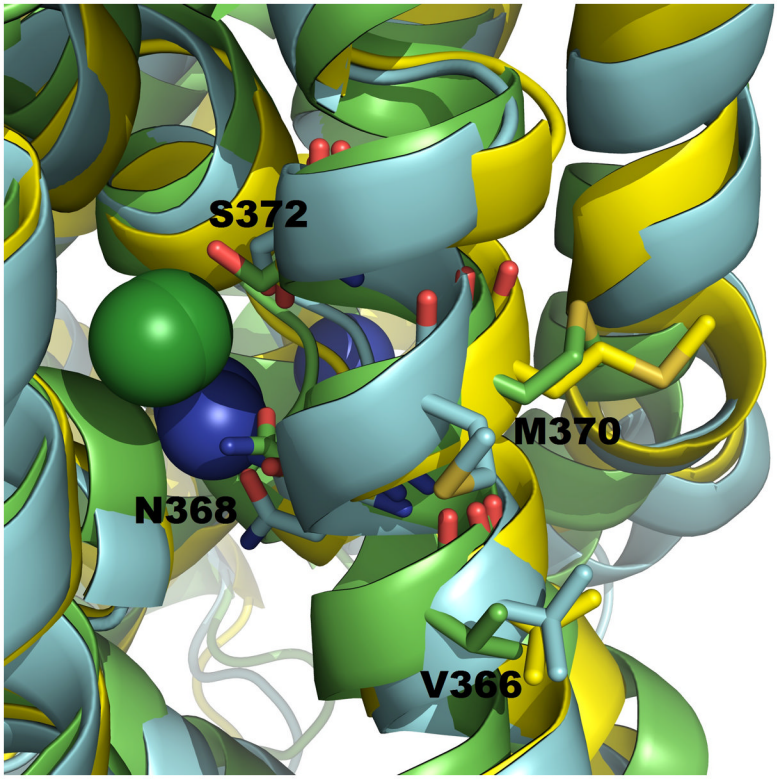

Figure 7.

Structure of TMH VII and ion binding sites in hSERT homology model. The protein conformation (green) was the input homology model structure with no molecular dynamics simulation or minimization. The blue (3 ns) and yellow (23 ns) conformations show the protein after placement in a realistic POPC membrane/water/NaCl environment and after energy minimization as described in Materials and Methods. First, position restraints were held on the membrane while the membrane and water were equilibrated, then the system including the protein was minimized using steepest descent (10000 steps or until the maximum force in the system was less than 1.000 kJ mol^{-1} nm^{-1}). After the simulation system was constructed and minimized (see Methods), the system was subjected to a 40 ns molecular dynamics simulation. The different conformations are superimposed with the input structure revealing potential mobility in the helix around this region, in particular a potentially unstable helix in the turn above M370, and significant movement of M370 itself (see 3ns–23ns). The green and blue spheres represent the location of the chloride ion and the sodium ions, respectively.

Table 1

K_i values for inhibition of [^{3}H]5-HT transport at TMH VII mutants

	K_i, nM ± SEM					
	hSERT	**V366S**	**V367I**	**M370L**	**S375A**	**T381S**
Citalopram	5.0 ± 1.0	3.0 ± 1.0	3.0 ± 2.0	7.0 ± 2.0	2.0 ± 1.0	3.0 ± 1.0
Fluoxetine	20 ± 9.0	13 ± 6.0	40 ± 30	20 ± 17	30 ± 20	12 ± 2.0
Imipramine	3.0 ± 1.0	1.0 ± 0.1	4.0 ± 1.0	4.0 ± 2.0	4.0 ± 3.0	2.0 ± 0.2
Sertraline	5.0 ± 2.0	1.0 ± 0.2	5.0 ± 1.0	3.0 ± 1.0	3.0 ± 1.0	1.0 ± 0.2
Venlafaxine	30 ± 7.0	20 ± 1.0	30 ± 8.0	30 ± 17	8.0 ± 1.0	25 ± 16
RTI-55	7.0 ± 2.0	3.0 ± 2.0	16 ± 6.0	16 ± 2.0	9.0 ± 6.0	7.0 ± 1.0
MMAI	800 ± 300	2000 ± 700	3000 ± 1000	900 ± 100	2000 ± 400	3000 ± 900
DCA	200 ± 100	500 ± 200	300 ± 100	70 ± 20	200 ± 20	400 ± 200

RTI-55, 3β-(4-iodophenyl)tropane-2β-carboxylic acid methyl ester; MMAI, 5-Methoxy-6-methyl-2-aminoindan; DCA, 3,4-dichloroamphetamine.